Cell

An RNA Sensor for Intracellular Mg^{2+}

Michael J. Cromie,[1,2] Yixin Shi,[1,2,3] Tammy Latifi,[1] and Eduardo A. Groisman[1,*]
[1] Howard Hughes Medical Institute, Department of Molecular Microbiology, Washington University School of Medicine, 660 South Euclid Avenue, Campus Box 8230, St. Louis, MO 63110, USA
[2] These authors contributed equally to this work.
[3] Present address: Arizona State University, The Biodesign Institute, Center for Infectious Diseases and Vaccinology, College of Liberal Arts and Sciences, School of Life Sciences, PO Box 874501, Tempe, AZ 85287, USA.
*Contact: groisman@borcim.wustl.edu
DOI 10.1016/j.cell.2006.01.043

SUMMARY

Most RNA molecules require Mg^{2+} for their structure and enzymatic properties. Here we report the first example of an RNA serving as sensor for cytoplasmic Mg^{2+}. We establish that expression of the Mg^{2+} transporter MgtA of *Salmonella enterica* serovar Typhimurium is controlled by its 5′ untranslated region (5′UTR). We show that the 5′UTR of the *mgtA* gene can adopt different stem-loop structures depending on the Mg^{2+} levels, which determine whether transcription reads through into the *mgtA* coding region or stops within the 5′UTR. We could recapitulate the Mg^{2+}-regulated transcription using a defined in vitro transcription system with RNA polymerase as the only protein component. The initiation of *mgtA* transcription responds to extracytoplasmic Mg^{2+} and its elongation into the coding region to cytoplasmic Mg^{2+}, providing a singular example in which the same ligand is sensed in different cellular compartments to regulate disparate steps in gene transcription.

INTRODUCTION

Mg^{2+} is the most abundant divalent cation in biological systems (Romani and Scarpa, 2000). It is essential for a wide variety of cellular activities, functioning as a cofactor in ATP-dependent enzymatic reactions and as stabilizer of membranes and ribosomes (Reinhart, 1988). While cells maintain cytoplasmic Mg^{2+} levels within a narrow range, little is known about the mechanisms by which cells sense Mg^{2+} and achieve Mg^{2+} homeostasis. In this paper, we describe an RNA sensor that specifically responds to cytoplasmic Mg^{2+} to control expression of a high-affinity Mg^{2+} transporter.

The organism that is best understood in terms of Mg^{2+} homeostasis is the Gram-negative bacterium *Salmonella enterica* serovar Typhimurium, which harbors a Mg^{2+}-responding two-component regulatory system (i.e., PhoP/PhoQ) (Groisman, 2001) and three Mg^{2+} transporters (i.e., CorA, MgtA, and MgtB) (reviewed in Smith and Maguire, 1998). The PhoP/PhoQ system consists of the Mg^{2+} sensor PhoQ, which responds to extracytoplasmic Mg^{2+} by modifying the phosphorylated state of the DNA binding protein PhoP (see Groisman, 2001 for a review). When *Salmonella* experiences low Mg^{2+}, the PhoQ protein favors phosphorylation of the PhoP protein, resulting in expression of PhoP-activated genes, and, when it faces high Mg^{2+}, PhoQ promotes dephosphorylation of phospho-PhoP, which represses transcription of PhoP-activated genes (Castelli et al., 2000; Chamnongpol et al., 2003; Chamnongpol and Groisman, 2000; Montagne et al., 2001; Soncini et al., 1996).

The Mg^{2+} transporter CorA mediates both the influx and efflux of Mg^{2+} and does not exhibit sequence similarity to MgtA and MgtB, which are 50% identical to each other and solely mediate Mg^{2+} influx (reviewed in Smith and Maguire, 1998). MgtA and MgtB also differ from CorA in that transcription of the *mgtA* and *mgtB* genes is directly regulated by the PhoP protein in response to extracytoplasmic Mg^{2+} sensed by the PhoQ protein (Soncini et al., 1996; Yamamoto et al., 2002; Zwir et al., 2005), whereas expression of CorA responds to neither Mg^{2+} nor the PhoP/PhoQ system (Chamnongpol and Groisman, 2002). The *mgtA* gene appears to be regulated by an additional Mg^{2+}-sensing device because chromosomal *mgtA* transcription still responded to Mg^{2+} in a strain lacking the Mg^{2+} sensor PhoQ and harboring PhoP*, a variant form of the PhoP protein that expresses PhoP-activated genes independently of the Mg^{2+} levels in the cell's surroundings (Chamnongpol and Groisman, 2000), and because luciferase activity originating from a plasmid-borne *mgtA* promoter-*lux* fusion was still regulated by Mg^{2+} in *phoP* and *phoQ* mutants (Tao et al., 1998).

Riboswitches are metabolite-sensing regulatory elements located within RNAs (Brantl, 2004; Nudler and Mironov, 2004; Winkler and Breaker, 2003). Naturally occurring riboswitches have been identified that respond to enzyme cofactors (Nahvi et al., 2004; Winkler et al., 2002), amino acids (Epshtein et al., 2003; Sudarsan et al., 2003), nucleotides (Mandal et al., 2003), and sugars (Winkler et al., 2004) and that sense temperature changes (Johansson et al., 2002). In this paper, we provide the first example of a cation-responsive riboswitch. By conducting in vivo gene-expression assays, RNA structure probing,

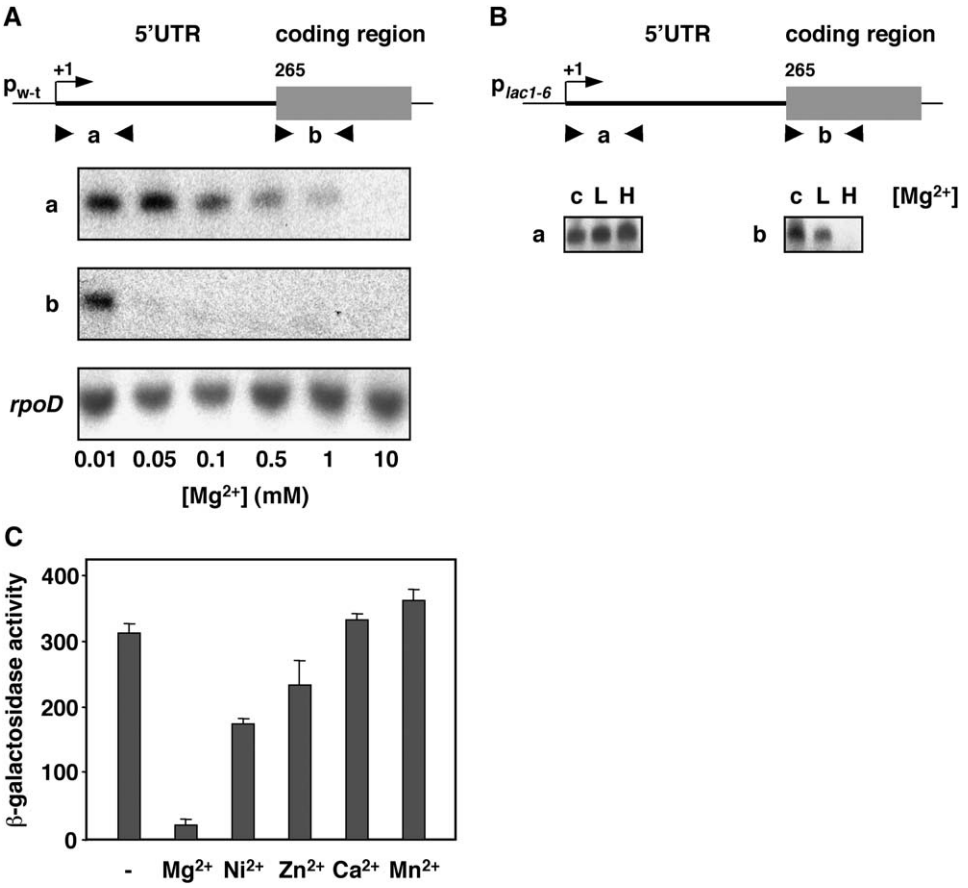

Figure 1. The 5′UTR and Coding Regions of the *mgtA* mRNA Are Differentially Regulated by Mg^{2+}

(A) Reverse transcription PCR analysis of the *mgtA* mRNA levels synthesized by wild-type *Salmonella* (14028s) grown for 4 hr in N-minimal medium (pH 7.4) with the indicated concentrations of Mg^{2+} (to final OD_{600} of ca. 0.3 for bacteria grown in 10 μM Mg^{2+} and ca. 0.5 for bacteria grown in 10 mM Mg^{2+}). The fragments generated by reverse transcription PCR with primer pair a correspond to nucleotides 1–100 of the 5′UTR of *mgtA* (thin line at top), and those generated with primer pair b correspond to nucleotides 1–100 of the *mgtA* coding region (block at top). The primer pair *rpoD* represents nucleotides 1–100 of the coding region of the *rpoD* gene, whose expression is not regulated by the PhoP/PhoQ system and was used as control.

(B) Reverse transcription PCR analysis of the *mgtA* mRNA levels synthesized by Plac1 strain YS929 harboring the p_{lac1-6} promoter instead of the wild-type *mgtA* promoter grown in N-minimal medium (pH 7.4) with 10 μM (L) or 10 mM (H) Mg^{2+}. The fragments were generated with primer pairs a and b indicated in (A). Chromosomal DNA template (c) was used as a positive control for the PCR reactions.

(C) β-galactosidase activities (Miller units) from Plac0 strain YS774 harboring the p_{lac1-6} promoter and a *lacZYA* transcriptional fusion to the *mgtA* gene in bacteria grown in N-minimal medium (pH 7.4) with 10 μM Mg^{2+} (L) plus the cations indicated in the figure added at 25 μM. Data correspond to mean values from three independent experiments performed in quadruplicate. Error bars correspond to the standard deviation (and are shown only if larger than the resolution of the figure).

mutational analysis, and in vitro transcription experiments, we establish that the 5′ untranslated region (5′UTR) of the *mgtA* mRNA functions as a Mg^{2+}-sensing regulatory element that controls production of the MgtA protein by determining whether transcription reads through into the *mgtA* coding region or stops within the 5′UTR.

RESULTS AND DISCUSSION

The 5′UTR and Coding Regions of the *mgtA* mRNA Are Differentially Regulated by Mg^{2+}

We examined the *mgtA* mRNA levels of wild-type *Salmonella* that had been grown in the presence of different Mg^{2+} concentrations by conducting reverse transcription PCR (RT-PCR) with primers corresponding to the first 100 nucleotides of the 264 nucleotide 5′UTR or the first 100 nucleotides of the coding region. No mRNA for the 5′UTR or coding region was detected in cells grown in 10 mM Mg^{2+} (Figure 1A), which was expected because the PhoP/PhoQ system is not active at such a high Mg^{2+} concentration (Garcia Vescovi et al., 1996). The mRNA corresponding to the 5′UTR was present in cells experiencing 1 mM Mg^{2+}, and its levels increased as the concentration of Mg^{2+} used to grow the bacteria decreased (Figure 1A). On the other hand, the mRNA corresponding to the coding region was detected in organisms grown

in 10 μM Mg^{2+} but not in those grown in ≥50 μM Mg^{2+} (Figure 1A). These findings are specific for *mgtA* as the mRNA levels corresponding to the *rpoD* gene (which was used as control) were not affected by the levels of Mg^{2+} in the media (Figure 1A). Moreover, they indicate that the *mgtA* transcript reaches the coding region only when *Salmonella* experiences very low Mg^{2+} concentrations, even though *mgtA* transcription is initiated at Mg^{2+} concentrations that are 100-fold higher.

To explore the basis for the differences in the *mgtA* mRNA levels exhibited by the 5′UTR and the coding region, we investigated a strain in which the wild-type *mgtA* promoter was replaced by a derivative of the *lac* promoter—designated $p_{lac1\text{-}6}$—that is independent of the cAMP receptor protein (i.e., CRP) (Liu et al., 2004) and the PhoP protein (see Figure S1A in the Supplemental Data available with this article online) and does not respond to Mg^{2+} (Figure S1B). We found similar mRNA levels for the 5′UTR in low and high Mg^{2+} (Figure 1B), which is consistent with transcription being promoted by the $p_{lac1\text{-}6}$ promoter. In contrast, there were strikingly higher mRNA levels for the coding region in organisms grown in low Mg^{2+} than in those grown in high Mg^{2+} (Figure 1B). These results indicate that Mg^{2+} can regulate *mgtA* expression even when transcription is initiated by a heterologous promoter.

mgtA Transcription Elongation Specifically Responds to Mg^{2+}

We inquired whether transcription elongation into the *mgtA* coding region responds to cations other than Mg^{2+} by using strain YS774, with the PhoP-independent $p_{lac1\text{-}6}$ promoter instead of the wild-type *mgtA* promoter and a *lacZYA* transcriptional fusion in the *mgtA* coding region. We found that Mn^{2+} and Ca^{2+}, which are cations that repress transcription initiation by the wild-type promoter (Garcia Vescovi et al., 1996), did not repress *mgtA* transcription in strain YS774 (Figure 1C) (see Experimental Procedures). Likewise, Ni^{2+} and Co^{2+}, which inhibit MgtA-mediated Mg^{2+} uptake (Snavely et al., 1989), failed to turn off *mgtA* expression or did so only at concentrations that were toxic to the bacterium (Figure 1C and data not shown). Zn^{2+}, which is an excellent inhibitor of Mg^{2+} transport by the MgtA protein (Snavely et al., 1989), reduced *mgtA* expression less than 2-fold at concentrations at which Mg^{2+} reduces expression 25-fold (Figure 1C). These results indicate that Mg^{2+} specifically controls whether transcription of the *mgtA* gene proceeds into the coding region.

The 5′UTR of *mgtA* Is Necessary and Sufficient to Respond to Mg^{2+}

To determine whether the 5′UTR of the *mgtA* transcript is required for PhoQ-independent regulation by Mg^{2+}, we evaluated *mgtA* transcription in isogenic derivatives of a *phoP*phoQ*::Tn*10* strain, which encodes the PhoP* variant that functions in the absence of the Mg^{2+} sensor PhoQ (Chamnongpol and Groisman, 2000). A strain derivative where the 100 bp sequence corresponding to positions

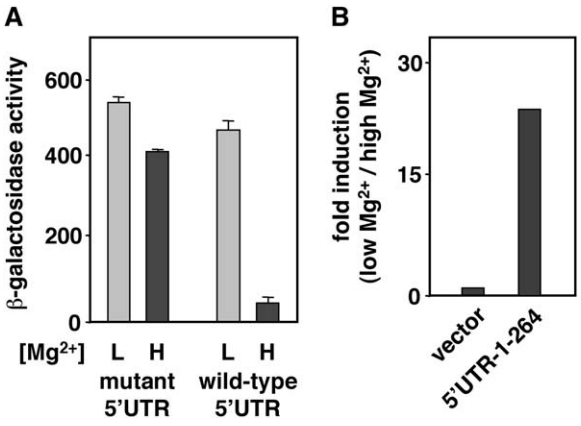

Figure 2. The 5′UTR of *mgtA* Is Required for Mg^{2+}-Regulated PhoQ-Independent Expression of the *mgtA* Gene and Confers Mg^{2+} Regulation to a Plasmid-Linked Heterologous Promoter

(A) β-galactosidase activity (Miller units) expressed by bacteria harboring an *mgtA-lac* fusion grown in N-minimal medium (pH 7.4) with 10 μM (L) or 10 mM (H) Mg^{2+} was determined in isogenic *phoP*phoQ*::Tn*10* derivatives with a mutant 5′UTR in which nucleotides 148–247 were replaced by the 84 bp "scar" sequence (see Experimental Procedures) (YS782) or harbored the wild-type 5′UTR (EG10238). Data correspond to mean values from at least three independent experiments performed in duplicate. Error bars correspond to the standard deviation (and are shown only if larger than the resolution of the figure).

(B) Ratio of the β-galactosidase activity (Miller units) expressed by wild-type *Salmonella* (14028s) harboring a plasmid with the *mgtA* 5′UTR behind the $p_{lac1\text{-}6}$ promoter and before the *E. coli lacZ* gene (pYS1010) or the plasmid vector (pYS1000) grown in N-minimal medium (pH 7.4) with 10 μM (L) versus 10 mM (H) Mg^{2+}. The fold induction of β-galactosidase activity was calculated by dividing the β-galactosidase activity of cells grown in 10 μM (L) Mg^{2+} by the β-galactosidase activity of cells grown in 10 mM (H) Mg^{2+}. Data correspond to mean values from at least three independent experiments performed in duplicate. The actual values of β-galactosidase activity are presented in Table S3.

148 to 247 of the 5′UTR was substituted by the 84 bp "scar" sequence (see Experimental Procedures) did not respond to Mg^{2+} and constitutively expressed *mgtA* (Figure 2A), which was in contrast to the strain with the wild-type 5′UTR (Figure 2A).

We established that the *mgtA* 5′UTR is sufficient to confer Mg^{2+} responsiveness because the levels of β-galactosidase activity were regulated by Mg^{2+} in a wild-type *Salmonella* strain harboring a plasmid with the sequence corresponding to the 264 nucleotide 5′UTR of *mgtA* between the $p_{lac1\text{-}6}$ promoter and the *Escherichia coli lacZ* gene but not in an isogenic strain with a plasmid lacking the *mgtA* 5′UTR (Figure 2B). The ability to confer Mg^{2+} responsiveness appears to be specific to the *mgtA* 5′UTR because cells with an isogenic plasmid containing the 5′UTR of the *ugtL* gene, which is also transcriptionally controlled by the PhoP/PhoQ system (Hilbert et al., 1999; Shi et al., 2004), produced similar levels of β-galactosidase activity in low and high Mg^{2+} (Figure S2). Taken together, these results demonstrated that the 5′UTR of *mgtA* is necessary and sufficient to confer Mg^{2+} regulation.

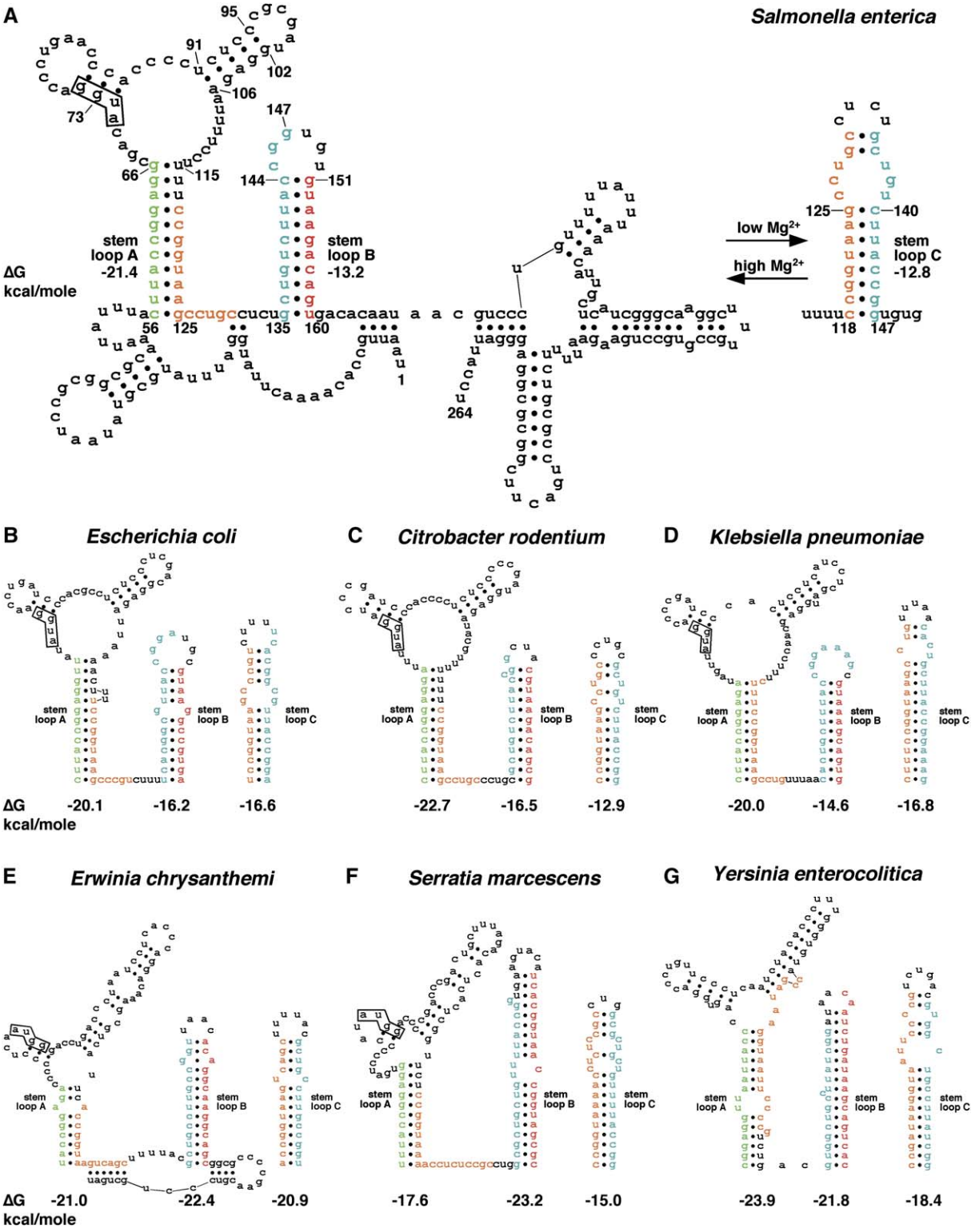

Figure 3. Predicted Secondary Structure of the Phylogenetically Conserved *mgtA* 5′UTR

(A) Schematic representation of the secondary structure of the 264 nucleotide *mgtA* 5′UTR from *Salmonella enterica* serovar Typhimurium as predicted by the Mfold program. Left: stem loops A and B, which are postulated to form in high Mg^{2+}. Right: stem loop C, which is predicted to form in low Mg^{2+}. Sequences in color represent regions involved in stem structures. The predicted energy for stem loops A, B, and C is presented underneath.

A Possible Regulatory Mechanism Suggested by the Phylogenetically Conserved Structure of the *mgtA* 5′UTR

We used the Mfold program (http://www.bioinfo.rpi.edu/applications/mfold/) to predict the secondary structure that might be adopted by the *mgtA* 5′UTR and identified two potential stem-loop structures that we termed A and B (Figure 3A). The stem in A would result from pairing nucleotides 56–66 to nucleotides 115–125, and the stem in B from pairing nucleotides 135–144 to nucleotides 151–160 (Figure 3A). Further analysis revealed that an alternative stem-loop structure—termed C—could be formed by pairing nucleotides 118–125 from the right arm of stem A to nucleotides 140–147 from the left arm of stem B plus three nucleotides from loop B (Figure 3A).

Investigation of the microbial genome databases indicated the presence of *mgtA* homologs in eight additional Gram-negative species. In six of these species—*E. coli*, *Citrobacter rodentium*, *Klebsiella pneumoniae*, *Erwinia chrysanthemi*, *Serratia marcescens*, and *Yersinia enterocolitica*—the *mgtA* open reading frame was preceded by sequences that, upon transcription, could adopt stem-loop structures very similar to those described above for the *Salmonella mgtA* 5′UTR (Figures 3B–3G). The predicted stem regions of these species are highly conserved or have minor nucleotide substitutions that retain the ability to adopt the alternative stem-loop structures A plus B versus C. In addition to the stem loops A, B, and C, other regions of the 5′UTR are also conserved (Figure S3). For example, the AUGG sequence corresponding to positions 71–74 in the loop A of the *Salmonella* 5′UTR is found in six of the seven species, and the predicted stem-loop structure at positions 91–106 in the *Salmonella* 5′UTR is present in four of the species (Figure 3). This analysis suggests that expression of the *mgtA* gene might be controlled in a similar manner in these enteric bacteria, which is the case for *E. coli* because its *mgtA* 5′UTR conferred Mg^{2+} regulation when cloned in a plasmid between the $p_{lac1\text{-}6}$ promoter and the *E. coli lacZ* gene (Figure S2), like the *Salmonella mgtA* 5′UTR (Figure 2B).

Taken together with the data presented in the previous sections (Figure 1 and Figure 2), the analysis of the 5′UTR raised the possibility that *mgtA* expression is regulated by a transcription attenuation-like mechanism (Henkin and Yanofsky, 2002; Landick et al., 1996). Under this scenario, the *mgtA* 5′UTR might adopt different structures (i.e., stem loops A plus B versus C), which would be determined by the cytoplasmic Mg^{2+} levels, and result in transcription stopping within the 5′UTR or proceeding into the *mgtA* coding region.

Table 1. Mg^{2+}-Regulated Expression of the *mgtA* Gene in Strains with 5′UTRs of Different Lengths

	β-Galactosidase Activity (Miller Units)	
Strains	Low Mg^{2+}	High Mg^{2+}
Plac0	253 ± 26	24 ± 5
Plac32	431 ± 34	45 ± 3
Plac76	312 ± 4	236 ± 2
Plac126	0	0
Plac158	645 ± 34	399 ± 12

β-galactosidase activity (Miller units) expressed by strains harboring a *mgtA-lac* transcriptional fusion transcribed from the $p_{lac1\text{-}6}$ promoter located at different positions within the 5′UTR: −11 (Plac0, YS774), 32 (Plac32, YS802), 76 (Plac76, YS779), 126 (Plac126, YS824), and 158 (Plac158, YS803) (Figure S4). Bacteria were grown in N-minimal medium (pH 7.4) with 10 μM (low) or 10 mM (high) Mg^{2+}. Data correspond to mean values from two independent experiments performed in duplicate. Errors correspond to standard deviation.

Potential Role of the Different Stem-Loop Structures in *mgtA* Expression

We constructed a set of isogenic strains with a chromosomal *lacZYA* fusion in the *mgtA* coding region, lacking the PhoP-regulated wild-type *mgtA* promoter and harboring the $p_{lac1\text{-}6}$ promoter at different positions within the *mgtA* 5′UTR sequence. By generating shorter transcripts that were precluded from forming particular stem-loop structures (Figure 3A), we hoped to gain insight into which structures might be associated with transcription stopping before versus continuing into the *mgtA* coding region.

When transcription was initiated at position 32, *mgtA* expression was responsive to Mg^{2+} (Table 1) as in strain Plac1 (Figure 1B), which starts transcription at the same position as the wild-type promoter, arguing that the first 31 nucleotides of the 5′UTR are not necessary for Mg^{2+} regulation of *mgtA* expression. (The transcription start site for the *mgtA* gene in the generated strains was verified experimentally by S1 mapping [Figure S4]; *mgtA* expression was also regulated by Mg^{2+} in strain Plac0, where *mgtA* transcription starts 11 nucleotides upstream of the wild-type start site [Table 1].) When transcription began at position 76, *mgtA* expression was constitutively active (Table 1). The 5′UTR in strain Plac76 lacks the sequences that make up the left arm of stem A. According to the Mfold program, this would preclude formation of stem loop A but not stem loop C, which would be favored over stem loop B. When transcription started at position 126, there was no

(B–G) Predicted stem-loop structures A, B, and C corresponding to the potential 5′UTRs for the *mgtA* gene from *Escherichia coli*, *Citrobacter rodentium*, *Kelbsiella pneumoniae*, *Erwinia chrysanthemi*, *Serratia marcescens*, and *Yersinia enterocolitica*. Sequences in color represent regions involved in stem-loop structures. The predicted energy for the three stem loops A, B, and C is presented underneath. Note conservation of AUGG sequence of loop A in all species but *Y. enterocolitica* and of the short stem loop within loop A in *S. enterica*, *E. coli*, *C. rodentium*, and *K. pneumoniae*. Other conserved regions are shown in Figure S3.

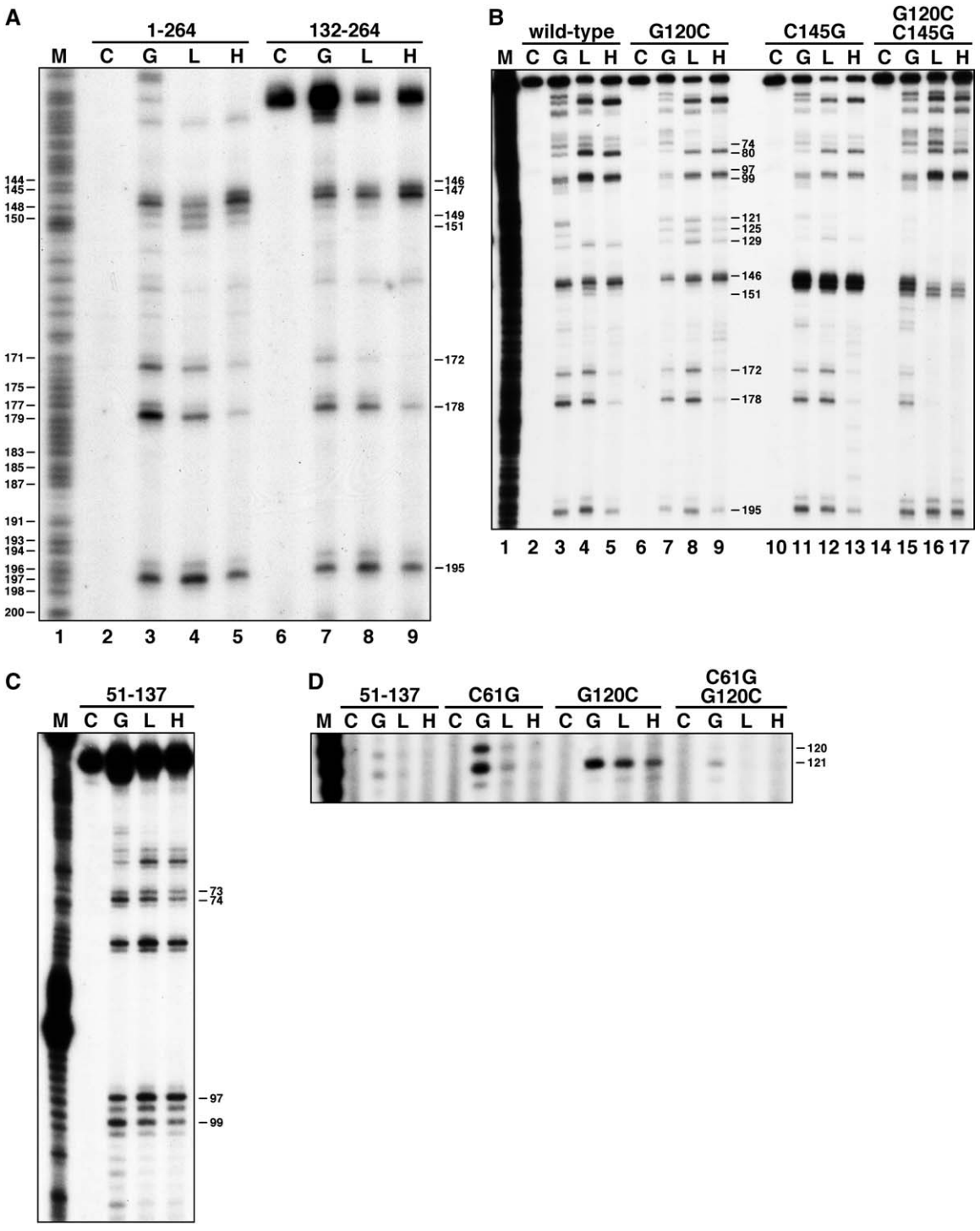

Figure 4. RNase T1 Probing of Wild-Type or Mutant Derivatives of the *mgtA* 5′UTR Affected in Stem Loops C or A

(A) RNase T1 cleavage of the full-length *mgtA* 5′UTR (1–264; lanes 2–5) or of a fragment lacking the stem loop A region (132–264; lanes 6–9) of the *mgtA* 5′UTR following denaturation and incubation with 0.35 (L) or 3.5 mM (H) Mg^{2+} as described in Experimental Procedures. C corresponds to untreated RNA, G to T1-treated RNA that was previously denatured, and M to a C-plus-U marker lane. A 6% polyacrylamide gel was used to separate the products.

(B) RNase T1 cleavage of the full-length wild-type 264 nucleotide 5′UTR or derivatives with the G120C, C145G, or G120 and C145G substitutions. The RNA samples were treated and run as described in Experimental Procedures and in (A), which also has the description of C, G, and M.

mgtA expression (Table 1). The 5′UTR in strain Plac126 could not form stem loops A or C, but the ability to form stem loop B remained unaltered (Figure 3A). This suggests that stem loop B may be the structure formed in high Mg^{2+} and be responsible for transcription stopping before the *mgtA* coding region. These results also imply that formation of stem loop C, being the alternative to stem loops A plus B, might be favored in low Mg^{2+}. Finally, when transcription initiated at position 158, *mgtA* expression was constitutively high (Table 1). The 5′UTR in strain Plac158 lacks the sequences that make up stem loops A, B, and C, indicative that sequences within the first 157 nucleotides of the 5′UTR are necessary for Mg^{2+}-regulated expression of the *mgtA* gene. In sum, these data suggest that formation of stem loops B and C is associated with transcription stopping and reading through into the *mgtA* coding region, respectively.

Mg^{2+} Modifies the Structure of the *mgtA* 5′UTR

We asked whether Mg^{2+} alters the structure of the *mgtA* 5′UTR and whether the structures adopted by the 5′UTR resemble those predicted by the Mfold program (Figure 3A). We used T7 RNA polymerase to synthesize the full-length 264 nucleotide *mgtA* 5′UTR, and, following incubation in the presence of different concentrations of Mg^{2+}, we treated the RNA with RNases or chemicals to probe the *mgtA* 5′UTR structure.

Treatment with RNase T1, which cleaves unpaired G residues, revealed that Mg^{2+} differentially affects the accessibility of several guanosines. For example, G151 was cleaved much more in low Mg^{2+} than in high Mg^{2+} (Figure 4A, lanes 3–5), suggesting that G151 is base paired in high Mg^{2+} but not in low Mg^{2+}, which is in agreement with the model presented in Figure 3A. This is in contrast to the similar T1 cleavage observed in high and low Mg^{2+} at the nearby G149 (Figure 4A, lanes 3–5), a nucleotide predicted to stay unpaired under both conditions (Figure 3A). On the other hand, G146 and G147 were cleaved more in high Mg^{2+} than in low Mg^{2+} (Figure 4A, lanes 3–5), indicating that they are unpaired and accessible to T1 in high Mg^{2+} but not as much in low Mg^{2+}. This is consistent with the model in which G146 and G147 are part of loop B in high Mg^{2+} and stem C in low Mg^{2+} (Figure 3A). We also observed more T1 cleavage in low than in high Mg^{2+} at G73 and G74 in the stem loop A region (Figure 4B, lanes 3–5) and also at G172, G178, and G195 (Figure 4A, lanes 3–5), downstream of stem loop B (Figure 3A).

RNase V1 recognizes residues that are in a somewhat helical conformation and can be used to detect base-paired nucleotides. Although Mg^{2+} affects V1 activity (Lowman and Draper, 1986), we obtained useful information about base-paired regions in the *mgtA* 5′UTR (Figures S5B and S5C) and determined that V1 cleavage at C127 was enhanced in high Mg^{2+} compared to low Mg^{2+} (Figure S5C). Chemical treatment with 1-cyclohexyl-3-(2-morpholinoethyl)-carbodiimide metho-p-toluene sulfonate (CMCT), which alkylates unpaired uridines and (to a lesser extent) unpaired guanosines, and with dimethyl sulfate (DMS), which alkylates unpaired adenosines and cytidines, resulted in modifications (Figures S5D and S5E) generally supporting the predictions made by the model (Figure 3A). On the other hand, we found that G97, U128, and G129 were modified by CMCT in low more than in high Mg^{2+} (Figure S5D), which was also the case for DMS modification of C126 and C127 (Figure S5D), in agreement with the results of V1 treatment. These data argue that nucleotides 126–129 are not single stranded in high Mg^{2+} in the tertiary structure of the *mgtA* 5′UTR, which is in contrast to the prediction made by Mfold (Figure 3A). Cumulatively, the results presented in this section demonstrate that Mg^{2+} can modify the structure of the *mgtA* 5′UTR.

Mutations that Affect Stem Loop C Formation Abolish Low-Mg^{2+}-Induced *mgtA* Expression

To test the model wherein stem loop C is favored in low Mg^{2+} and promotes *mgtA* transcription whereas stem loops A plus B are favored in high Mg^{2+} and inhibit *mgtA* expression (Figure 3A), we investigated both the ability of mutant derivatives of the *mgtA* 5′UTR to mediate Mg^{2+}-regulated gene expression and whether the structure of the mutant RNAs is modified by Mg^{2+}.

We constructed a mutant with the C145G single-nucleotide substitution in the loop sequence of stem loop B that is predicted to be part of the left arm of stem C, so that formation of stem C would be disrupted without interfering with the formation of stem B (Figure 3A). In this mutant, *mgtA* expression was off regardless of the Mg^{2+} concentration (Table 2). An almost identical phenotype was displayed by the G120C mutant (Table 2), which is also expected to be defective in formation of stem C (Figure 3A). On the other hand, a double mutant harboring both the C145G and G120C substitutions displayed Mg^{2+}-regulated *mgtA* expression similar to that of the wild-type 5′UTR (Table 2). The restoration of activity in the double mutant supports a model in which G120 normally base pairs with C145 (Figure 3A) and formation of stem loop C is required for *mgtA* expression in low Mg^{2+}. Although G120 is predicted to pair with C61 in high Mg^{2+} (Figure 3A), a mutant with the C61G substitution retained near wild-type regulation of *mgtA* expression (Table 2), possibly because stem A is still formed due to base stacking of G residues (Figure 3A).

We probed the structure of the mutant 5′UTRs with RNase T1, focusing on those guanosines that are differentially affected by Mg^{2+} in the wild-type 5′UTR (Figure 4A, lanes 3–5). We determined that, whereas G151 is cleaved

(C) RNase T1 cleavage of the 51–137 nucleotide stem loop A region of the *mgtA* 5′UTR. The RNA samples were treated and run as described in Experimental Procedures and in (A).

(D) RNase T1 cleavage of the 51–137 nucleotide stem loop A region of the *mgtA* 5′UTR or derivatives with the C61G, G120C, or C61G and G120 substitutions. The RNA samples were treated and run as described in Experimental Procedures and in (A).

Table 2. Mg^{2+}-Regulated Expression Mediated by the *mgtA* 5′UTR or Mutant Derivatives

Plasmid	β-Galactosidase Activity (Miller Units)	
	Low Mg^{2+}	High Mg^{2+}
pYS1000 (vector)	9615 ± 192	5161 ± 226
pYS1010 (*mgtA*-5′UTR)	798 ± 26	77 ± 3
pYS1010-C61G	692 ± 57	156 ± 11
pYS1010-G120C	3 ± 3	0
pYS1010-C145G	16 ± 5	3 ± 3
pYS1010-C61G-G120C	4 ± 3	3 ± 2
pYS1010-G120C-C145G	876 ± 115	117 ± 14
pYS1010-C61G-G120C-C145G	607 ± 100	157 ± 7
pYS1010-mut91-95	76 ± 2	41 ± 2
pYS1010-mut91-95-mut102-106	641 ± 48	44 ± 4
pYS1010-1-178	605 ± 44	382 ± 50

β-galactosidase activity (Miller units) expressed by wild-type *Salmonella* (14028s) harboring the plasmid vector pYS1000, plasmid pYS1010 with the *Salmonella mgtA* 5′UTR located behind the p_{lac1-6} promoter and before the *E. coli lacZ* gene, or derivatives of plasmid pYS1010 with nucleotide substitutions or deletions in the *mgtA* 5′UTR region. Strains were grown in N-minimal medium (pH 7.4) with 10 μM (L) or 10 mM (H) Mg^{2+}. Data correspond to mean values of four experiments. Errors correspond to standard deviation.

in low Mg^{2+} in the wild-type 5′UTR (Figure 4B, lanes 3–5), there was no cleavage at either high or low Mg^{2+} in the G120C mutant (Figure 4B, lanes 7–9). The C145G mutant 5′UTR behaves like the G120C mutant in that it fails to express the *mgtA* gene (Table 2). However, the profile of the C145G mutant RNA was different from both those of the wild-type and G120C RNAs in that there was much enhanced T1 cleavage at G147 and G149 (Figure 4B, lanes 11–13). The RNAs corresponding to the G120C and the C145G single mutants were not cleaved at the conserved G73 and G74 (Figure 4B, lanes 7–9 and 11–13), but the RNA for the Mg^{2+}-responding G120C C145G double mutant showed the Mg^{2+}-regulated cleavage displayed by the wild-type RNA at these nucleotides (Figure 4B, lanes 15–17 and 3–5). Yet the T1 cleavage pattern of the G120C C145G double mutant RNA was not entirely like that of the wild-type because there was no cleavage at G146 and because G151 was cleaved to a similar extent in low and high Mg^{2+} (Figure 4B, lanes 15–17). Collectively, these results demonstrate that the ability to form stem loop C is necessary for Mg^{2+}-regulated *mgtA* transcription as mutants that affect formation of stem loop C are unable to express the *mgtA* gene and exhibit an altered RNA structure.

Stem Loop A Is Critical for Mg^{2+} Sensing

The ΔGs predicted for stem loops B and C are very similar (i.e., −12.7 and −12.8 kcal/mole, respectively), suggesting that the decision over which of these two structures forms is probably made by a different region of the 5′UTR, most likely in response to Mg^{2+}. We hypothesized that loop A may be one such region because parts of this loop are highly conserved in other enteric species (Figure 3A) and because some of the conserved regions are differentially cleaved by T1 in the presence of Mg^{2+} (Figure 4B, lanes 3–5). Thus, we investigated the phenotype of mutant loop A derivatives, the ability of Mg^{2+} to alter the structure of stem loop A when present by itself, and whether Mg^{2+}-promoted changes in stem loops B and C depend on the presence of stem loop A.

The Mfold program predicts the formation of a short stem from the pairing of nucleotides ^{91}UCUCC^{95} to ^{102}GGAGA^{106} (Figure 3A). We constructed a mutant disrupted in such a stem by replacing the ^{91}UCUCC^{95} sequence by ^{91}AGAGG^{95} and found that the resulting 5′UTR lost the ability to respond to Mg^{2+}, promoting constitutive *mgtA* transcription, albeit at levels lower than the wild-type 5′UTR when experiencing low Mg^{2+} (Table 2). The formation of this short stem and its role in Mg^{2+} sensing is supported by the phenotype of a double mutant with the ^{91}AGAGG^{95} and ^{102}CCUCU^{106} substitutions, which regained Mg^{2+} regulation of *mgtA* expression (Table 2) possibly due to the renewed ability to form a stem.

We probed the structure of stem loop A by examining the T1 cleavage pattern of an RNA corresponding to nucleotides 51–137 of the 264 nucleotide 5′UTR. We observed enhanced accessibility to T1 in low Mg^{2+} at the conserved G73 and G74, and also for G99 (Figure 4C). These results indicate that Mg^{2+} can affect the structure of the loop A region even in the absence of sequences located upstream and downstream of stem loop A. We then sought evidence for the existence of the predicted stem in stem loop A (i.e., nucleotides 56–66 pairing to nucleotides 115–125) by comparing the T1 cleavage pattern of the wild-type stem loop A RNA to those corresponding to RNAs with nucleotide substitutions in this region. There was no cleavage in low or high Mg^{2+} at G120 or G121 in the wild-type stem A RNA (Figure 4D), consistent with these nucleotides being base paired (Figure 3A). However, cleavage could be detected at both of these residues in the RNA prepared from the C61G mutant (Figure 4D), which is anticipated to disrupt stem A (Figure 3A). Likewise, there was strong cleavage at G121 in the RNA prepared from the G120C mutant (Figure 4D). On the other hand, there was no cleavage at G121 in the C61G G120C double mutant (Figure 4D), presumably because stem A could reform. These data support the existence of stem A and demonstrate that Mg^{2+} can affect the structure of the stem loop A RNA when present by itself.

We have shown above that Mg^{2+} alters the accessibility of RNase T1 to G151 (Figure 4A, lanes 3–5), consistent with the notion that G151 may be part of stem B in high Mg^{2+} but unpaired in low Mg^{2+} (Figure 3A). We asked whether stem loop A was necessary for this change in stem B by comparing the T1 cleavage pattern of the full-length 264 nucleotide *mgtA* 5′UTR to that of a derivative containing only the 132–264 region, which lacks the stem

loop A sequences. We found no T1 cleavage at G151 or at the nearby G149 in either high or low Mg^{2+} in the latter RNA (Figure 4A, lanes 7–9), suggesting that the stem loop A is required for the Mg^{2+}-promoted changes in the loop B region.

In sum, our data demonstrate that stem loop A is required for Mg^{2+} sensing and for the Mg^{2+}-promoted changes taking place in stem loops B and C. While our results do not exclude the possibility that regions other than stem loop A may also participate in Mg^{2+} sensing, it is likely that, as the stem loop A region of the 5′UTR is transcribed, it traps the 5′UTR RNA into distinct structures depending on the Mg^{2+} concentration that ultimately determine whether transcription reads through into the *mgtA* coding region.

Mg^{2+} Inhibits Transcription Elongation beyond the *mgtA* 5′UTR In Vitro

To examine Mg^{2+}-regulated transcription elongation across the *mgtA* 5′UTR, we set up an in vitro transcription system consisting of *E. coli* RNA polymerase σ^{70} holoenzyme, linear DNA templates harboring the $p_{lac1\text{-}6}$ promoter (Liu et al., 2004), and different concentrations of Mg^{2+}. A transcription assay with a template containing the first 260 nucleotides of the *E. coli lacZ* coding region resulted in a transcript whose levels increased as the Mg^{2+} concentration increased (Figure 5A, left panel), which is consistent with the Mg^{2+} dependency of the in vitro transcription reaction (Niyogi and Feldman, 1981). In contrast, when we used a template containing the same promoter and identical upstream sequences but harboring the full-length wild-type 5′UTR of the *mgtA* gene, two bands were observed: a large one representing the readthrough transcript, the amount of which decreased as the Mg^{2+} concentration increased (Figure 5A, right panel), and a small one corresponding to a truncated product of approximately 220 nucleotides (Figure 5A, right panel). Thus, higher levels of the readthrough transcript were obtained at low Mg^{2+} even though the $p_{lac1\text{-}6}$ promoter functions better at high Mg^{2+}. Changes in the relative levels of the readthrough and truncated transcripts were observed in the range of Mg^{2+} concentrations reported for *Salmonella* growing in defined media (Froschauer et al., 2004).

The site where transcription stops is unusual in that the sequences preceding it do not have the typical features of Rho-independent terminators (i.e., a GC-rich RNA hairpin followed by a poly-U sequence (Landick et al., 1996)) and in that the generation of a truncated product did not require the Rho protein. This raised the possibility of the truncated product resulting from RNA-mediated cleavage as demonstrated for the glucosamine-6-phosphate-responding riboswitch (Winkler et al., 2004), as opposed to originating from transcription stopping. To distinguish between these two possibilities, we conducted the in vitro transcription reaction with the 5′UTR-containing template and then added ^{32}pCp and T4 RNA ligase, which resulted in labeling of the truncated product (Figure 5B). This indicates the presence of a free 3′OH group in the generated RNA and suggests that the truncated RNA was likely produced as a result of early transcription termination or pausing because ribozymes that yield free 2′ and 3′ hydroxyl groups are typically larger than the 220 nucleotide *mgtA* 5′UTR (Jacquier, 1996). Consistent with this notion, a single product was obtained when the 5′UTR was synthesized in vitro by T7 RNA polymerase instead of *E. coli* RNA polymerase (Figure 5C). This product was of the same size as that corresponding to the readthrough transcript generated with *E. coli* RNA polymerase. Moreover, when the *E. coli* RNA polymerase was used to transcribe the template with the *mgtA* 5′UTR, there was no delay in the appearance of the truncated product relative to the readthrough product as would be expected for a maturation reaction (data not shown). Furthermore, addition of Mg^{2+} did not promote degradation of the readthrough transcript generated in vitro (data not shown). Cumulatively, these results demonstrate that the *mgtA* 5′UTR responds to Mg^{2+} by affecting the ability of RNA polymerase to stop transcription, which may explain the small *mgtA*-derived RNA detected in vivo in both *Salmonella* (unpublished data) and *E. coli* (Kawano et al., 2005).

The Region Downstream of Stem Loop B Is Required for Mg^{2+}-Regulated *mgtA* Expression

We hypothesized that sequences beyond position 160 in the 5′UTR (Figure 3A) might be required for Mg^{2+}-regulated *mgtA* expression for the following reasons: first, Mg^{2+} affected T1 cleavage at positions G172, G178, and G195 (Figure 4A, lanes 3–5) and V1 cleavage at U193 (Figure S5B); second, this region is conserved among enteric species (Figure S3); and third, transcription termination takes place in this region (Figure 5A, right panel). Consistent with this notion, a strain harboring a derivative of the 5′UTR with the sequence corresponding to positions 1 to 178 constitutively expressed the *mgtA* gene (Table 2). This suggests that sequences downstream of stem loop B participate in Mg^{2+} sensing and/or transcription stopping.

Concluding Remarks

Expression of the Mg^{2+} transporter MgtA is governed at two distinct steps: First, the initiation of *mgtA* transcription is regulated by the PhoP protein, whose activity is controlled by the sensor PhoQ in response to extracytoplasmic Mg^{2+} (Garcia Vescovi et al., 1996), and second, the early stopping of *mgtA* transcription is controlled by its 5′UTR, which responds to cytoplasmic Mg^{2+} (Figure 6). This dual control may enable *Salmonella* to exert differential regulation of those determinants directly affecting cytoplasmic Mg^{2+} (i.e., the Mg^{2+} transporters MgtA and MgtB), which are transcriptionally controlled by the same regulatory system (i.e., PhoP/PhoQ) governing expression of the determinants mediating modifications in the bacterial cell envelope. Indeed, expression of the PhoP-regulated *mgtCB* operon, which encodes the inner-membrane protein MgtC and the Mg^{2+} transporter MgtB, appears to be controlled in an *mgtA*-like fashion as *mgtCB* transcription also responds to Mg^{2+} in the absence of the Mg^{2+}

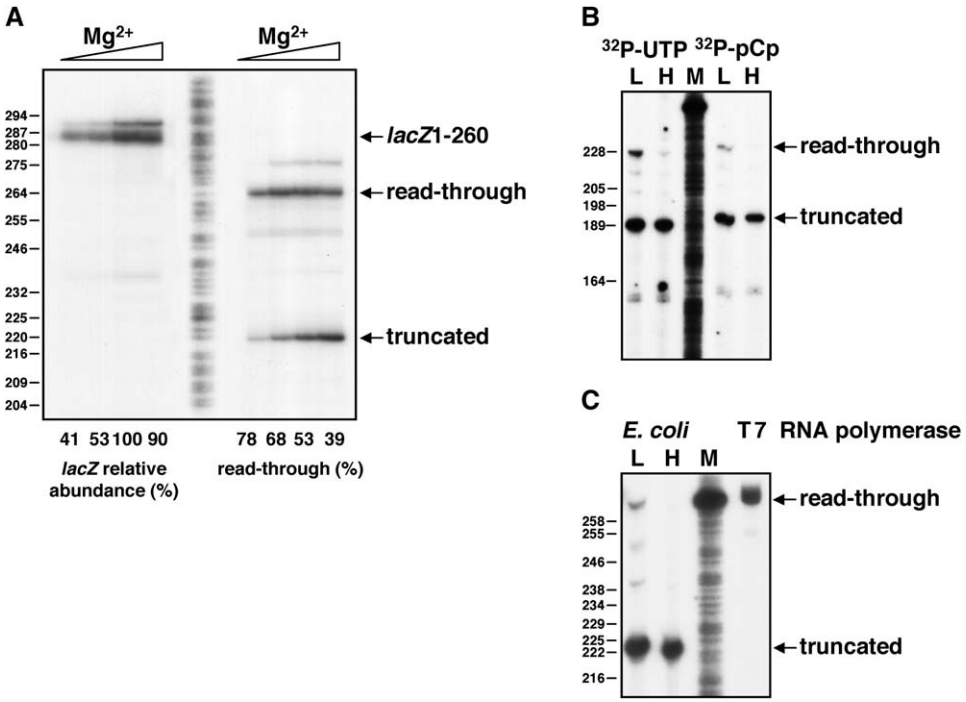

Figure 5. Mg^{2+} Promotes Transcription Stopping within the 5′UTR of *mgtA* In Vitro

(A) In vitro transcription of templates corresponding to the first 260 nucleotides of the *lacZ* coding region driven by the $p_{lac1\text{-}6}$ promoter (left panel) or harboring the $p_{lac1\text{-}6}$ promoter and the full-length wild-type *mgtA* 5′UTR sequence (right panel) was conducted as described in Experimental Procedures. Arrow indicates the transcripts synthesized from reactions containing (from left to right) 0.35, 0.7, 1.4, or 3.5 mM Mg^{2+}. The *lacZ* relative abundance was calculated by the formula (intensity of transcript at a given Mg^{2+} concentration)/(intensity of the most highly expressed transcript) × 100. The percent of readthrough product was calculated by the formula (intensity of readthrough transcript at a given Mg^{2+} concentration)/(intensity of readthrough transcript at a given Mg^{2+} concentration + intensity of truncated transcript in such Mg^{2+} concentration) × 100. The intensities were first corrected to account for the number of Us in each transcript. With the same formula used to calculate the relative abundance of *lacZ*, we determined that, for reactions containing 0.35, 0.7, 1.4, or 3.5 mM Mg^{2+}, the relative abundance of the readthrough product was 67%, 100%, 94%, and 67%, respectively, and for the truncated product was 18%, 47%, 81%, and 100%, respectively. The ladder corresponds to a PCR product generated with primers 4443 and ^{32}P-labeled primer 4445 and degraded by the Maxam and Gilbert reaction.

(B) In vitro transcription of a template corresponding to the Plac32 strain YS802 and harboring the $p_{lac1\text{-}6}$ promoter with the full-length wild-type *mgtA* 5′UTR sequence was conducted in buffer containing 0.35 (L) or 3.5 (H) mM Mg^{2+}. Readthrough and truncated products are indicated by arrows. The products were labeled with ^{32}pCp as described in Experimental Procedures.

(C) In vitro transcription of a template harboring the $p_{lac1\text{-}6}$ promoter and the full-length wild-type *mgtA* 5′UTR sequence conducted in buffer containing 0.35 (L) or 3.5 (H) mM Mg^{2+} using RNA polymerase from *E. coli* (left) or phage T7 (right). The reactions were performed as described in Experimental Procedures.

sensor PhoQ protein in a process that requires the 5′UTR of the *mgtCB* operon (unpublished data).

When *Salmonella* experiences a low-Mg^{2+} environment, *mgtA* is the first PhoP-activated gene that is transcribed (unpublished data), which may reflect the organism's effort to maintain physiological levels of cytoplasmic Mg^{2+}. Once the MgtA protein is produced, it will mediate internalization of Mg^{2+}, which will eventually bind to the *mgtA* 5′UTR to shut off MgtA expression. This regulatory design allows for rapid uptake of Mg^{2+} and at the same time makes MgtA an arbiter of its own expression (Figure 6).

The dual control described for *mgtA* is in contrast to the vast majority of genes that are controlled by riboswitches, which are typically regulated solely by their respective riboswitches (Brantl, 2004; Nudler and Mironov, 2004; Winkler and Breaker, 2003). Yet it is not unprecedented for genes subjected to attenuation-like regulation, as expression of the *trp* biosynthetic genes of *E. coli* is determined both by the tryptophan-responding TrpR protein binding to the *trp* promoter-operator region and by a transcription attenuation mechanism that senses charged $tRNA^{Trp}$ (Bennett and Yanofsky, 1978; Yanofsky, 2004). However, the *mgtA* regulation differs from that of the *trp* genes in that in the former case the same ligand (i.e., Mg^{2+}) acts at two different cell compartments (i.e., the periplasm and the cytoplasm) to control gene expression, whereas in the latter case different molecules (i.e., tryptophan and $tRNA^{Trp}$) do so in the same compartment (i.e., the cytoplasm).

Mg^{2+} has been known to be a critical ion for the structure and biochemical properties of many RNAs (Draper et al., 2005). We now report that Mg^{2+} can regulate gene expression by modifying the structure of the *mgtA* 5′UTR. To our knowledge, the 5′UTR of the Mg^{2+} transporter *mgtA* gene constitutes the first example of a

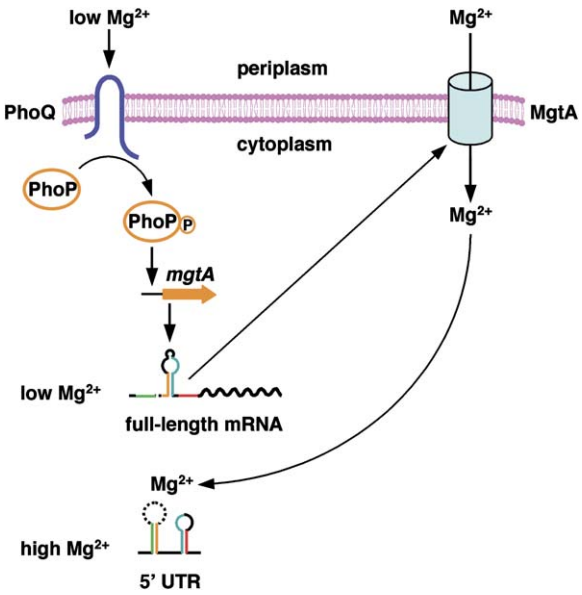

Figure 6. Model for Regulation of the *Salmonella* MgtA Mg^{2+} Transporter

When *Salmonella* experiences a low-Mg^{2+} environment, the sensor PhoQ responds to extracytoplasmic Mg^{2+} by promoting phosphorylation of the DNA binding protein PhoP, which binds to the *mgtA* promoter and initiates *mgtA* transcription. If cytoplasmic Mg^{2+} levels are above a certain threshold, Mg^{2+} binding to the *mgtA* 5′UTR results in the formation of stem-loop structures that promote transcription stopping within the 5′UTR. Once the cytoplasmic Mg^{2+} concentration goes below a certain level, an alternative stem-loop structure is formed, which allows readthrough into the *mgtA* coding region. Production of the MgtA protein allows internalization of Mg^{2+}, the concentration of which will increase, resulting in binding to the *mgtA* 5′UTR and the shutting off of MgtA expression.

riboswitch that responds to a metal ion. It is likely that additional ion-regulated riboswitches exist, as suggested by in silico analyses of several putative ion transporters (Barrick et al., 2004; Merino and Yanofsky, 2005).

EXPERIMENTAL PROCEDURES

Bacterial Strains, Plasmids, and Growth Conditions

Bacterial strains and plasmids used in this study are listed in Table S1. All *Salmonella enterica* serovar Typhimurium strains used in this study were derived from the wild-type strain 14028s. MudJ (also known as MudI1734) is a derivative of bacteriophage Mu (Castilho et al., 1984) that was used to generate *lacZYA* transcriptional fusions to the *mgtA* gene. Phage P22-mediated transductions were performed as described (Davis et al., 1980). Bacteria were grown at 37°C in Luria-Bertani (LB) broth or in N-minimal medium (pH 7.4) (Snavely et al., 1991), supplemented with 0.1% casamino acids, 38 mM glycerol, and different concentrations of $MgCl_2$. The ability of Mn^{2+}, Ni^{2+}, Co^{2+}, Ca^{2+}, or Zn^{2+} to repress *mgtA* transcription was investigated in N-minimal medium supplemented with 10 μM Mg^{2+} plus the cation of interest at 25 μM. This concentration was chosen because it was sufficient for Mg^{2+}-promoted repression of *mgtA* transcription. When necessary, antibiotics were added to final concentrations of 50 μg/ml for ampicillin, 20 μg/ml for chloramphenicol, 50 μg/ml for kanamycin, and 12.5 μg/ml for tetracycline. *E. coli* strain DH5α was used as host for the preparation of plasmid DNA. Strain and plasmid constructions are presented in Supplemental Experimental Procedures. The "scar" sequence, which corresponds to the 84 bp that remain after removing the Cm^R cassette generated by the one-step disruption procedure (Datsenko and Wanner, 2000), is as follows: 5′-TGTGTAGGCTGGAGCTGCTTCGAAGTTCCTATACTTTCTAGGAATAGGAACTTCGGAATAGGAACTAAGGAGGATATTCATATG-3′.

Reverse Transcription PCR

Total RNA was isolated with the MasterPure RNA Purification Kit (EPICENTRE) according to the manufacturer's specifications. Reverse transcription was carried out with TaqMan Reverse Transcription Reagents (Applied Biosystems, Roche), cDNA was synthesized by using 0.5 μg total RNA as template according to the manufacturer's specifications, and PCR was carried out with 2× TaqPCR Master Mix (QIAGEN) and 1.25 μCi [α-^{32}P]dCTP per reaction for 26 thermocycles to amplify the first 100 bp of the *mgtA* 5′UTR using primers 4443 and 4446 or to amplify the first 100 bp of the *mgtA* coding region using primers 4439 and 4440. As a control, primers 6179 and 6180 were used to amplify the first 100 bp of the *rpoD* coding region, whose expression does not respond to changes in the concentration of Mg^{2+}.

β-Galactosidase Assays

β-galactosidase assays were carried out in duplicate or triplicate, as indicated in the figure or table legends, and the activity was determined as described (Miller, 1972).

Enzymatic and Chemical Probing of the *mgtA* 5′UTR RNA Structure

The *mgtA* 5′UTR RNA was synthesized with T7 RiboMAX Express Large Scale RNA Production Systems (Promega) according to the manufacturer's specifications using PCR-generated products as templates. The PCR products were generated using DNA from wild-type *Salmonella* strain 14028s and the following primers: 6427 and 6432 for the 51–137 template, 6429 and 4445 for the 132–264 template, and 4443 and 4445 for the 1–264 template.

RNase probing of the *mgtA* 5′UTR secondary structure was carried out as described (Knapp, 1989), with the following modifications. Cleavage with RNase T1 was carried out using the 3′ ^{32}pCp-labeled RNA generated from the T4 RNA ligase reaction (England et al., 1980). A tube containing 11.8 μl of H_2O and 3 μl of 3′ ^{32}pCp-labeled RNA (corresponding to ~1.2 μg) was heated at 95°C for 5 min, put on ice for 30 s, and then placed at room temperature for 2 min. Then, we added 2 μl of 3.5 or 35 mM $MgCl_2$, 1 μl 2 M KCl, and 0.2 μl 1 M Tris (pH 7.0) and incubated at 37°C for 30 min. Then, we added 0.04 U RNase T1 (diluted from a 1 U/μl stock solution to 0.2 U/μl with reaction buffer, which had the same composition described above). The tubes were incubated at 37°C for 15 min. Forty microliters of inactivation/precipitation buffer (Ambion) was added, and the tubes were incubated at −20°C for 15 min. The RNA was pelleted by centrifugation at 14,000 rpm for 15 min, and the pellet was washed with 75% ethanol and air dried. Ten microliters of gel loading buffer II (Ambion) was added, mixed, and heated to 95°C for 5 min. Three microliters was used to load 6% acrylamide/7.5 M urea sequencing gel. The gel was run for different amounts of time. Cleavage with RNase V1 was performed as described above for T1, except that we used 0.01 U RNase V1 in a total volume of 20 μl of RNA solution containing 1.2 μg of 3′ ^{32}pCp-labeled RNA.

Chemical modification of the RNA with DMS was carried out as follows: One microliter of RNA solution (corresponding to 5 μg) was mixed with 134 μl of H_2O, incubated at 95°C for 5 min, cooled on ice for 30 s, and placed at room temperature for 5 min. Forty microliters of 1 M HEPES, 5 μl of 2 M KCl, and 20 μl of 3.5 or 35 mM $MgCl_2$ were added and incubated at 37°C for 30 min. One microliter of DMS was added, and the reaction mixture was incubated at 37°C for 5 min. Twenty microliters of 3 M NaAc (pH 5.5) was added. Then, 600 μl cold ethanol was added, and the tube was vortexed and kept on dry ice for 15 min. The RNA was pelleted by centrifugation at

14,000 rpm for 15 min, and the pellet was washed with 75% ethanol and air dried. The products were reverse transcribed using SuperScript II RNase H$^-$ Reverse Transcriptase (Invitrogen) according to the manufacturer's specifications, separated using 7.5 M urea polyacrylamide gel electrophoresis, and detected by autoradiography. The cleavage sites were determined by using a DNA sequencing ladder generated from a PCR product amplified with primers 4443 and ^{32}P-labeled 4445 and degraded by the Maxam and Gilbert reaction. DMS modification of the denatured RNA was carried out in a similar fashion except that we used 2 μl of RNA solution (corresponding to 10 μg), which was mixed with 230.5 μl of H_2O, incubated at 95°C for 5 min, cooled on ice for 30 s, and placed at room temperature for 5 min. We then added 60 μl of 1 M HEPES (pH 8.0) and 7.5 μl of 2 M KCl. We incubated at 90°C for 1 min, added 1 μl of DMS, and incubated at 90°C for 30 s. Thirty microliters of 3 M NaAc (pH 5.5) was added as well as 900 μl of cold ethanol. The tube was vortexed and kept on dry ice for 15 min. The RNA was pelleted by centrifugation at 14,000 rpm for 15 min, and the pellet was washed with 75% ethanol and air dried. The products were reverse transcribed as described above.

Chemical modification of the RNA with CMCT was carried out as follows: One microliter of RNA solution (corresponding to 5 μg) was mixed with 123.75 μl H_2O, incubated at 95°C for 5 min, cooled on ice for 30 s, and placed at room temperature for 5 min. 7.5 μl of 1 M NaB_4O_7 (pH 8.0), 3.75 μl of 2 M KCl, and 15 μl of 3.5 or 35 mM $MgCl_2$ were added and incubated at 37°C for 30 min. Fifty microliters of 42 mg/ml solution of CMCT (in H_2O) was added, and the reaction mixture was incubated at 37°C for 5 min. Twenty microliters of 3 M NaAc (pH 5.5) was added. Then, 600 μl cold ethanol was added, and the tube was vortexed and kept on dry ice for 15 min. The RNA was pelleted by centrifugation at 14,000 rpm for 15 min, and the pellet was washed with 75% ethanol and air dried. The products were reverse transcribed by using SuperScript II RNase H$^-$ Reverse Transcriptase (Invitrogen) according to the manufacturer's specifications, separated using 7.5 M urea polyacrylamide gel electrophoresis, and detected by autoradiography. The cleavage sites were determined by using a DNA sequencing ladder generated from a PCR product amplified with primers 4443 and ^{32}P-labeled 4445 and degraded by the Maxam and Gilbert reaction. CMCT modification of the denatured RNA was carried out in the same fashion except that the 7.5 μl of 1 M NaB_4O_7 (pH 8.0) and 3.75 μl of 2 M KCl (i.e., no $MgCl_2$) was added and the incubation was carried out at 90°C for 1 min instead of 37°C for 30 min. Then, 50 μl of 42 mg/ml solution of CMCT (in H_2O) was added, and the incubations and treatments were carried out as described above.

In Vitro Transcription Assays Using *E. coli* RNA Polymerase

Linear DNA templates containing the p_{lac1-6} promoter region were generated by the PCR as follows: The control template that includes the first 260 nucleotide fragment of the *lacZ* gene was amplified from plasmid pYS1000 DNA using primers 5539 and 5910, and the template harboring the full-length *mgtA* 5′UTR was amplified using plasmid pYS1010 DNA and primers 5539 and 5511. Single-round in vitro transcription was carried out as described (Kajitani and Ishihama, 1983). Briefly, 1 unit of *E. coli* RNA polymerase σ^{70} holoenzyme (EPICENTRE) was incubated with 0.5 μg template DNA in 35 μl transcription buffer, which contains 100 mM Tris-HCl (pH 8.0), 100 mM NaCl, 0.2 mM EDTA, 0.2 mM DTT, 50 μg/ml BSA, and the indicated Mg^{2+} concentrations (i.e., 0.35, 0.7, 1.4, and 3.5 mM) at 37°C for 30 min to form open complexes. RNA synthesis was initiated by adding 15 μl of NTP-heparin mixture, which contained 0.32 mM ATP, CTP, GTP; 0.1 mM UTP; 3 μg heparin; and 2 μCi [α-^{32}P]UTP (Amersham). After a 10 min incubation at 37°C, transcripts were precipitated with one-tenth the volume of 3 M sodium acetate (pH 5.5) and three volumes of ethanol, separated in an 7.5 M urea polyacrylamide gel electrophoresis, and detected by autoradiography.

The kinetic analysis was carried out using the same conditions described above, except that the reaction volume was the number of time points × 50 μl. At each time point, 50 μl of the mixture was removed to a new Eppendorf tube, and transcription was stopped by the addition of ethanol.

In Vitro Transcription Using T7 RNA Polymerase

Linear full-length *mgtA* 5′UTR DNA templates carrying the T7 promoter region were generated by the PCR using chromosomal DNA from strain 14028s and primers 6712 and 5511. The in vitro transcription was carried out as follows: Five units of T7 RNA polymerase (EPICENTRE) was incubated with 0.5 μg template DNA in 20 μl transcription buffer, which contains 40 mM Tris-HCl (pH 7.5), 10 mM NaCl, 2 mM spermidine, 10 mM DTT, 6 mM Mg^{2+}, 0.5 mM ATP, CTP, GTP, 0.125 mM UTP, and 2 μCi [α-^{32}P]UTP. RNA synthesis was carried out by incubating this mixture at 37°C for 30 min. Transcripts were precipitated with ethanol, separated in 7.5 M urea polyacrylamide gel electrophoresis, and detected by autoradiography.

^{32}pCp Labeling of the 3′ End of the Generated RNA

T4 RNA ligase was purchased from New England Biolabs. The precipitated RNA product prepared for in vitro transcription experiments using *E.coli* RNA polymerase or T7 RNA polymerase was resuspended in 14 μl of H_2O, 10 μCi of ^{32}pCp (1 μl, Amersham), 2 μl of 10 mM ATP, 2 μl of 10X T4 RNA ligase reaction buffer, and 5 U (1 μl) of T4 RNA ligase. The reaction mixture was incubated at 4°C overnight, then treated once with an equal volume of phenol. Labeled RNA was precipitated with ethanol, separated in 7.5 M urea polyacrylamide gel electrophoresis, and detected by autoradiography.

S1 Nuclease Assay

The S1 nuclease protection assay was performed as described (Garcia Vescovi et al., 1996), with RNA harvested from mid-exponential-phase cultures (OD_{600} of 0.3–0.4) grown in 30 ml of N minimal medium (pH 7.4) containing 10 μM $MgCl_2$. Total RNA was isolated with SV Total RNA Isolation Kit (Promega) according to the manufacturer's specifications. Either primer 6074 or 4445 was labeled at the 5′ end by phosphorylation with [γ-^{32}P]ATP using T4 polynucleotide kinase (Invitrogen) as described (Kato et al., 2003), and a PCR product was generated using *Salmonella* chromosomal DNA as template and the following primer pairs: 6074 and 6075 or 4445 and 6075. The resulting labeled PCR products were used as probes as follows: The product generated with primers 6074 and 6075 was used with RNA prepared from wild-type (14028s), Plac0 (YS774), and Plac1 (YS929) strains; the product generated with primers 4445 and 6075 was used with RNA prepared from Plac32 (YS802), Plac76 (YS779), Plac 126 (YS824), and Plac158 (YS803) strains.

Supplemental Data

Supplemental Data include Supplemental Experimental Procedures, Supplemental References, four tables, and five figures and can be found with this article online at http://www.cell.com/cgi/content/full/125/1/71/DC1/.

ACKNOWLEDGMENTS

We would like to thank H. Huang and K. Hall for discussions; G. Storz, R. Landick, and C. Yanofsky for comments on an earlier version of the manuscript; and Melanie Spoor for the initial observation that triggered the experiments described in this paper. We would also like to thank three anonymous reviewers for their thoughtful comments. This work was supported in part by grant AI49561 from the National Institutes of Health to E.A.G., who is an Investigator of the Howard Hughes Medical Institute.

Received: April 18, 2005
Revised: November 23, 2005
Accepted: January 5, 2006
Published: April 6, 2006

REFERENCES

Barrick, J.E., Corbino, K.A., Winkler, W.C., Nahvi, A., Mandal, M., Collins, J., Lee, M., Roth, A., Sudarsan, N., Jona, I., et al. (2004). New RNA motifs suggest an expanded scope for riboswitches in bacterial genetic control. Proc. Natl. Acad. Sci. USA *101*, 6421–6426.

Bennett, G.N., and Yanofsky, C. (1978). Sequence analysis of operator constitutive mutants of the tryptophan operon of *Escherichia coli*. J. Mol. Biol. *121*, 179–192.

Brantl, S. (2004). Bacterial gene regulation: from transcription attenuation to riboswitches and ribozymes. Trends Microbiol. *12*, 473–475.

Castelli, M.E., García Véscovi, E.G., and Soncini, F.C. (2000). The phosphatase activity is the target for Mg2+ regulation of the sensor protein PhoQ in *Salmonella*. J. Biol. Chem. *275*, 22948–22954.

Castilho, B.A., Olfson, P., and Casdaban, M.J. (1984). Plasmid insertion mutagenesis and *lac* gene fusion with mini-Mu bacteriophage transposons. J. Bacteriol. *158*, 488–495.

Chamnongpol, S., and Groisman, E.A. (2000). Acetyl-phosphate-dependent activation of a mutant PhoP response regulator that functions independently of its cognate sensor kinase. J. Mol. Biol. *300*, 291–305.

Chamnongpol, S., and Groisman, E.A. (2002). Mg^{2+} homeostasis and avoidance of metal toxicity. Mol. Microbiol. *44*, 561–571.

Chamnongpol, S., Cromie, M., and Groisman, E.A. (2003). Mg^{2+} sensing by the Mg^{2+} sensor PhoQ of *Salmonella enterica*. J. Mol. Biol. *325*, 795–807.

Datsenko, K.A., and Wanner, B.L. (2000). One-step inactivation of chromosomal genes in *Escherichia coli* K-12 using PCR products. Proc. Natl. Acad. Sci. USA *97*, 6640–6645.

Davis, R.W., Bolstein, D., and Roth, J.R. (1980). Advanced Bacterial Genetics (Cold Spring Harbor, NY: Cold Spring Harbor Laboratory Press).

Draper, D.E., Grilley, D., and Soto, A.M. (2005). Ions and RNA folding. Annu. Rev. Biophys. Biomol. Struct. *34*, 221–243.

England, T.E., Bruce, A.G., and Uhlenbeck, O.C. (1980). Specific labeling of 3′ termini of RNA with T4 RNA ligase. Methods Enzymol. *65*, 65–74.

Epshtein, V., Mironov, A.S., and Nudler, E. (2003). The riboswitch-mediated control of sulfur metabolism in bacteria. Proc. Natl. Acad. Sci. USA *100*, 5052–5056.

Froschauer, E.M., Kolisek, M., Dieterich, F., Schweigel, M., and Schweyen, R.J. (2004). Fluorescence measurements of free [Mg^{2+}] by use of mag-fura 2 in *Salmonella enterica*. FEMS Microbiol. Lett. *237*, 49–55.

Garcia Vescovi, E., Soncini, F.C., and Groisman, E.A. (1996). Mg^{2+} as an extracellular signal: environmental regulation of *Salmonella* virulence. Cell *84*, 165–174.

Groisman, E.A. (2001). The pleiotropic two-component regulatory system PhoP-PhoQ. J. Bacteriol. *183*, 1835–1842.

Henkin, T.M., and Yanofsky, C. (2002). Regulation by transcription attenuation in bacteria: how RNA provides instructions for transcription termination/antitermination decisions. Bioessays *24*, 700–707.

Hilbert, F., Garcia-del Portillo, F., and Groisman, E.A. (1999). A periplasmic D-alanyl-D-alanine dipeptidase in the gram-negative bacterium *Salmonella enterica*. J. Bacteriol. *181*, 2158–2165.

Jacquier, A. (1996). Group II introns: Elaborate ribozymes. Biochimie *78*, 474–487.

Johansson, J., Mandin, P., Renzoni, A., Chiaruttini, C., Springer, M., and Cossart, P. (2002). An RNA thermosensor controls expression of virulence genes in *Listeria monocytogenes*. Cell *110*, 551–561.

Kajitani, M., and Ishihama, A. (1983). Determination of the promoter strength in the mixed transcription system: promoters of lactose, tryptophan and ribosomal protein L10 operons from *Escherichia coli*. Nucleic Acids Res. *11*, 671–686.

Kato, A., Latifi, T., and Groisman, E.A. (2003). Closing the loop: the PmrA/PmrB two-component system negatively controls expression of its posttranscriptional activator PmrD. Proc. Natl. Acad. Sci. USA *100*, 4706–4711.

Kawano, M., Reynolds, A.A., Miranda-Rios, J., and Storz, G. (2005). Detection of 5′- and 3′-UTR-derived small RNAs and cis-encoded antisense RNAs in *Escherichia coli*. Nucleic Acids Res. *33*, 1040–1050.

Knapp, G. (1989). Enzymatic approaches to probing of RNA secondary and tertiary structure. Methods Enzymol. *180*, 192–212.

Landick, R., Turnbough, C.L., and Yanofsky, C. (1996). Transcription attenuation. In *Escherichia coli* and *Salmonella* Cellular and Molecular Biology, F.C. Neidhardt, ed. (Washington, DC: ASM Press).

Liu, M., Tolstorukov, M., Zhurkin, V., Garges, S., and Adhya, S. (2004). A mutant spacer sequence between -35 and -10 elements makes the P_{lac} promoter hyperactive and cAMP receptor protein-independent. Proc. Natl. Acad. Sci. USA *101*, 6911–6916.

Lowman, H.G., and Draper, D.E. (1986). On the recognition of helical RNA by cobra venom V1 nuclease. J. Biol. Chem. *261*, 5396–5403.

Mandal, M., Boese, B., Barrick, J.E., Winkler, W.C., and Breaker, R.R. (2003). Riboswitches control fundamental biochemical pathways in *Bacillus subtilis* and other bacteria. Cell *113*, 577–586.

Merino, E., and Yanofsky, C. (2005). Transcription attenuation: a highly conserved regulatory strategy used by bacteria. Trends Genet. *21*, 260–264.

Miller, J.H. (1972). Experiments in Molecular Genetics (Cold Spring Harbor, NY: Cold Spring Harbor Laboratory Press).

Montagne, M., Martel, A., and Le Moual, H. (2001). Characterization of the catalytic activities of the PhoQ histidine protein kinase of *Salmonella enterica* serovar Typhimurium. J. Bacteriol. *183*, 1787–1791.

Nahvi, A., Barrick, J.E., and Breaker, R.R. (2004). Coenzyme B12 riboswitches are widespread genetic control elements in prokaryotes. Nucleic Acids Res. *32*, 143–150.

Niyogi, S.K., and Feldman, R.P. (1981). Effect of several metal ions on misincorporation during transcription. Nucleic Acids Res. *9*, 2615–2627.

Nudler, E., and Mironov, A.S. (2004). The riboswitch control of bacterial metabolism. Trends Biochem. Sci. *29*, 11–17.

Reinhart, R.A. (1988). Magnesium metabolism. A review with special reference to the relationship between intracellular content and serum levels. Arch. Intern. Med. *148*, 2415–2420.

Romani, A.M., and Scarpa, A. (2000). Regulation of cellular magnesium. Front. Biosci. *5*, D720–D734.

Shi, Y., Latifi, T., Cromie, M.J., and Groisman, E.A. (2004). Transcriptional control of the antimicrobial peptide resistance *ugtL* gene by the *Salmonella* PhoP and SlyA regulatory proteins. J. Biol. Chem. *279*, 38618–38625.

Smith, R.L., and Maguire, M.E. (1998). Microbial magnesium transport: unusual transporters searching for identity. Mol. Microbiol. *28*, 217–226.

Snavely, M.D., Florer, J.B., Miller, C.G., and Maguire, M.E. (1989). Magnesium transport in *Salmonella typhimurium*: $^{28}Mg^{2+}$ transport by the CorA, MgtA, and MgtB systems. J. Bacteriol. *171*, 4761–4766.

Snavely, M.D., Miller, C.G., and Maguire, M.E. (1991). The *mgtB* Mg^{2+} transport locus of *Salmonella typhimurium* encodes a P-type ATPase. J. Biol. Chem. *166*, 815–823.

Soncini, F.C., Garcia Vescovi, E., Solomon, F., and Groisman, E.A. (1996). Molecular basis of the magnesium deprivation response in

Salmonella typhimurium: identification of PhoP-regulated genes. J. Bacteriol. *178*, 5092–5099.

Sudarsan, N., Wickiser, J.K., Nakamura, S., Ebert, M.S., and Breaker, R.R. (2003). An mRNA structure in bacteria that controls gene expression by binding lysine. Genes Dev. *17*, 2688–2697.

Tao, T., Grulich, P.F., Kucharski, L.M., Smith, R.L., and Maguire, M.E. (1998). Magnesium transport in *Salmonella typhimurium*: biphasic magnesium and time dependence of the transcription of the *mgtA* and *mgtCB* loci. Microbiol. *144*, 655–664.

Winkler, W.C., and Breaker, R.R. (2003). Genetic control by metabolite-binding riboswitches. ChemBioChem *4*, 1024–1032.

Winkler, W.C., Cohen-Chalamish, S., and Breaker, R.R. (2002). An mRNA structure that controls gene expression by binding FMN. Proc. Natl. Acad. Sci. USA *99*, 15908–15913.

Winkler, W.C., Nahvi, A., Roth, A., Collins, J.A., and Breaker, R.R. (2004). Control of gene expression by a natural metabolite-responsive ribozyme. Nature *428*, 281–286.

Yamamoto, K., Ogasawara, H., Fujita, N., Utsumi, R., and Ishihama, A. (2002). Novel mode of transcription regulation of divergently overlapping promoters by PhoP, the regulator of two-component system sensing external magnesium availability. Mol. Microbiol. *45*, 423–438.

Yanofsky, C. (2004). The different roles of tryptophan transfer RNA in regulating trp operon expression in *E. coli* versus *B. subtilis*. Trends Genet. *20*, 367–374.

Zwir, I., Shin, D., Kato, A., Nishino, K., Latifi, T., Solomon, F., Hare, J.M., Huang, H., and Groisman, E.A. (2005). Dissecting the PhoP regulatory network of *Escherichia coli* and *Salmonella enterica.* Proc. Natl. Acad. Sci. USA *102*, 2862–2867.